Supporting Information for

Random Double-Cable Conjugated Polymers with Controlled Acceptor Contents for Single-Component Organic Solar Cells

Baiqiao Liu,[a,b,▽] Shijie Liang,[a,▽] Safakath Karuthedath,[c,g,▽] Chengyi Xiao,*[,a] Jing Wang,[d] Wen Liang Tan,[e] Ruonan Li,[b] Hao Li,[f] Jianhui Hou,[f] Zheng Tang,[d] Frédéric Laquai,[c] Christopher R. McNeill,[e] Yunhua Xu,*[,b] and Weiwei Li*[,a]

[a] Beijing Advanced Innovation Center for Soft Matter Science and Engineering & State Key Laboratory of Organic-Inorganic Composites, Beijing University of Chemical Technology, Beijing 100029, P. R. China. E-mail: xiaocy@mail.buct.edu.cn or liweiwei@iccas.ac.cn

[b] School of Physical Science and Engineering, Beijing Jiaotong University, Beijing 100044, P. R. China. E-mail: yhxu@bjtu.edu.cn

[c] King Abdullah University of Science and Technology (KAUST), KAUST Solar Center (KSC), Physical Sciences and Engineering Division (PSE), Material Science and Engineering Program (MSE), Thuwal 23955-6900, Kingdom of Saudi Arabia.

[d] Center for Advanced Low-dimension Materials, College of Materials Science and Engineering, Donghua University, Shanghai 201620, P. R. China.

[e] Department of Materials Science and Engineering, Monash University, Wellington Road, Clayton, Victoria 3800, Australia.

[f] State Key Laboratory of Polymer Physics and Chemistry, Beijing National Laboratory for Molecular Sciences, Institute of Chemistry, Chinese Academy of Sciences, Beijing 100190, P. R. China.

[g] Institute of Materials Research, Tsinghua Shenzhen International Graduate School, Tsinghua University, Shenzhen, 518055 China

[▽] Contributed equally to this work.

Contents

1. Materials and measurements

The synthetic procedures were performed under a nitrogen (N_2) atmosphere. Commercial chemicals (from *Sunatech Inc*., *J&K Chemical*, *Solarmer Materials Inc.,* and E*nergy Chemical*) were used as received. **M2** and **M3** were purchased from *Solarmer Materials Inc.* **M1** was prepared according to the literature procedures.[1]

^{1}H-NMR and ^{13}C-NMR spectra of intermedia products and monomers were recorded at 400 MHz and 100 MHZ on a Bruker AVANCE spectrometer. The Molecular weight was determined with GPC at 150 °C on a PL-GPC 220 system using a PL-GEL 13 μm Olexis column and 1,2,4-trichlorobenzene as the eluent against polystyrene standards. Optical absorption spectra were recorded on a HITACHI U-2910 spectrometer with a slit width of 2.0 nm and a scan speed of 800 nm/min. Cyclic voltammetry was performed under an inert atmosphere at a scan rate of 0.1 V/s and 1 M tetrabutylammonium hexafluorophosphate in acetonitrile as the electrolyte, a glassy-carbon working electrode coated with samples, a platinum-wire auxiliary electrode, and an Ag/AgCl as a reference electrode. Thermogravimetric analysis data were obtained from a Pyris6 (PerkinElmer), and DSC measurement was performed on a TAQ2000.

Solar cells. Photovoltaic devices with inverted configuration were made by spin-coating a ZnO sol-gel at 4000 rpm for 60 s onto pre-cleaned, patterned ITO substrates. The photoactive layers based on P1, P2, P3, or BHJ (PBDB-T:*s*-DCPIC, 1:2.26, *w*/*w*) were deposited by spin coating *o*-DCB:3%DIO solution. The thickness of the photoactive layers is about 50-70 nm. The thin films were then transferred into the N_2-filled glove box. MoO_3 (7 nm) and Ag (80 nm) were deposited by vacuum evaporation at ca. 4×10^{-5} Pa as the back electrode. The active area of the cells was 0.040 cm^2. The *J-V* curves were measured under AM1.5G illumination at 100 mW/cm^2 using an AAA solar simulator (XES-70S1, *SAN-EI Electric Co., Ltd*) calibrated with a standard photovoltaic cell equipped with a KG5 filter (certificated by the National Institute of Metrology) and a Keithley 2400 source-measure unit. The EQE data were obtained using a solar cell spectral response measurement system (QE-R3011, *Enli Technology Co. Ltd*). The film thickness data were obtained via a surface profilometer (Dektak XT, Bruker).

SCLC: The hole and electron mobility of P1, P2, P3, BHJ films (PBDB-T:*s*-DCPIC, 1:2.26, *w*/*w*) and PBDB-T:TPDIC blend films in OSCs were measured by space charge limited current (SCLC) measurement with the device configuration of ITO/PEDOT:PSS/active layer/MoO_3/Ag and ITO/ZnO/active layer/PDINN[2]/Ag, respectively. All film samples were prepared with the same measurement of the solar cell devices by spin-coating solutions in an N_2-filled glove box and thermally annealed for 10 min. The thickness of the photoactive layers is ~100 nm. The hole/electron mobilities were calculated with the *Mott-Gurney* equation in the SCLC region (slope = 2 in log*J* vs log*V* plots):[3, 4]

$$J = \frac{9}{8}\varepsilon_0\varepsilon_r\mu\frac{V^2}{L^3} \qquad \textbf{(eq. 1)}$$

Where ε_0 is the permittivity of the vacuum, ε_r is the dielectric constant of the polymer, and L is the thickness of the polymer layer.

Thermal stability test. For degradation experiments, the cells are placed in a hot platform at 80 °C in the N_2-filled glove box.

PL and EL. Photoluminescence (PL) and Electroluminescence (EL) spectra were taken using a Kymera-328I spectrograph and an EMCCD purchased from Andor Technology (DU970P).

***EQE*$_{EL}$**. EQE_{EL} measurements were done using a home-built setup using a Keithley 2400 to inject current into the solar cells. Emission photon-flux from the solar cells was recorded using a Si detector (Hamamatsu s1337-1010BQ) and a Keithley 6482 picometer.

sEQE (sensitivity EQE). The halogen light source (LSH-75, 250W, Newport) is converted into monochromatic light through a monochromator (CS260-RG-3-MC-A, Newport), and then the focused monochromatic light of 173 Hz is irradiated onto the device through a chopper (3502 Optical Chopper, Newport). The current generated by the device is amplified by the front-end current amplifier (SR570, Stanford Instruments) and lock-in amplifier (SR830, Stanford Instruments), to obtain the sensitivity EQE.

$$EQE(E) = \frac{fE}{\sqrt{4\pi\lambda kT}}\exp\left(-\frac{(E_{CT}+\lambda-E)^2}{4\lambda kT}\right) \quad \textbf{(eq. 2)}$$

$$EL(E) = EQE(E)\phi_{BB}(E)[\exp\left(\frac{qV}{kT}\right)-1] \quad \textbf{(eq. 3)}$$

E_{CT} is determined by sEQE measurement. According to the formula of gaussian relation between absorption (corresponding to EQE(E)) and energy (**eq. 2**), we can acquire the E_{CT} by fitting the low energy tails of EQE.[5, 6] The absorption spectra calculated from EL can be attached to the tails of the EQE spectra by utilizing the reciprocal relationship between EL and EQE (**eq. 3**).

GIWAXS measurements were performed at the SAXS/WAXS beamline at the Australian Synchrotron. 2D scattering patterns were recorded using a Pilatus 2M detector, with the sample-to-detector distance calibrated using a silver behenate reference standard. The sample and detector were enclosed in a vacuum chamber to suppress air scatter. Scattering patterns were measured as a function of the angle of incidence, with data shown acquired with an angle of incidence near the critical angle that maximized scattering intensity from the sample.

AFM. AFM images were recorded using a Digital Instruments Nanoscope IIIa multimode atomic force microscope in tapping mode under ambient conditions.

Transient absorption spectroscopy. TA spectroscopy was carried out using a homebuilt pump-probe setup as described in our previous papers.[7, 8] Two different configurations of the setup were used for either short delay, namely 200 fs to 8 ns experiments, or long delay, namely 1 ns to 300 μs delays. The output of a titanium: sapphire amplifier (Coherent LEGEND DUO, 4.5 mJ, 3 kHz, 100 fs) was split into three beams (2, 1, and 1.5 mJ). Two were used to separately pump two optical parametric amplifiers (OPA) (Light Conversion TOPAS Prime). The photophysical processes in this experiment were initiated by an ultrafast laser pulse generated by TOPAS 1 (pump pulses for short delay TA measurements) and were probed by a broad white light supercontinuum which was generated by sapphire crystal upon excitation with an 800 nm signal from titanium:sapphire amplifier.

An actively Q-switched Nd:YVO4 laser (InnoLas picolo AOT) provided the excitation light (532 nm) for long delay TA experiments which is triggered by an electronic delay generator triggered (Stanford Research Systems DG535). The electronic delay generator triggered by the TTL sync from the Legend DUO, allows to control of the delay between pump and probe with a jitter of roughly 100 ps.

Pump and probe beams were focused on the sample with the aid of proper optics. The transmitted fraction of the white light was guided to a custom-made prism spectrograph (Entwicklungsbüro Stresing) where it was dispersed by a prism onto a 512pixel NMOS linear image sensor (Hamamatsu S8381-512). The probe pulse repetition rate was 3 kHz, while the excitation pulses were mechanically chopped to 1.5 kHz (100 fs to 8 ns delays) or directly generated at 1.5 kHz frequency (1 ns to 300 μs delays), while the detector array was read out at 3 kHz. Adjacent diode readings corresponding to the transmission of the sample after excitation and in the absence of an excitation pulse were used to calculate $\Delta T/T$. Measurements were averaged over several thousand shots to obtain a good signal-to-noise ratio.

2. Synthesis of polymers

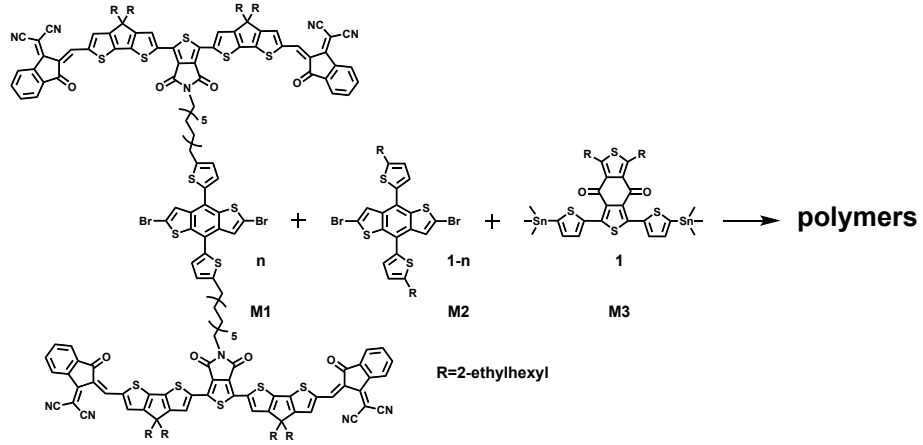

Scheme S1. Synthetic routes of the random double-cable polymers.

To a degassed solution of **M1** (n equ.), **M2** (1-n equ.) and **M3** (1 equ.) in toluene (5 mL), $Pd_2(dba)_3$ (0.03 equ.) and triphenylphosphine (0.12 equ.) were added. The mixture was stirred at 115 °C for 24 h, after which it was precipitated into methanol and filtered through a Soxhlet thimble. The polymer was extracted with acetone, hexane, dichloromethane, and chlorobenzene. The chlorobenzene was evaporated and the polymer was precipitated into acetone. The polymer was collected by filtering over a 0.45 μm PTFE membrane filter and dried in a vacuum oven to obtain polymers (yield ~70%) as a dark solid.

3. GPC, TGA, DSC and CV

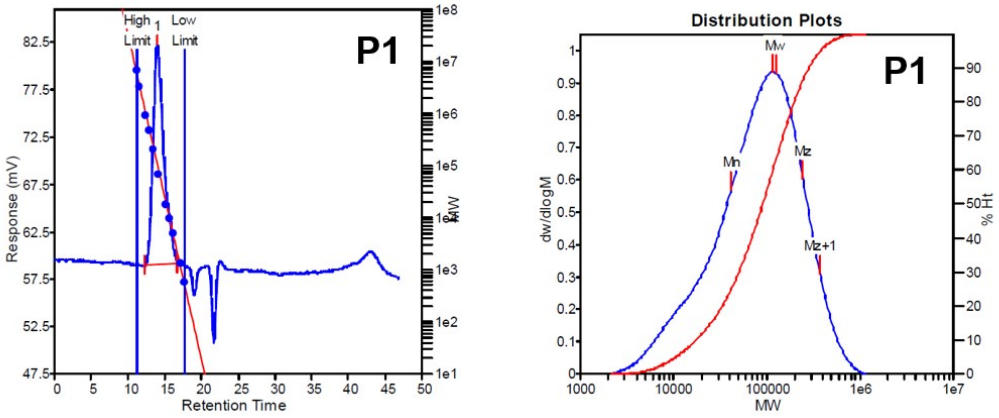

MW Averages

Peak No	Mp	Mn	Mw	Mz	Mz+1	Mv	PD
1	114718	41390	125633	244576	374269	109661	3.03535

Figure S1. GPC curve and molecular weight of **P1**.

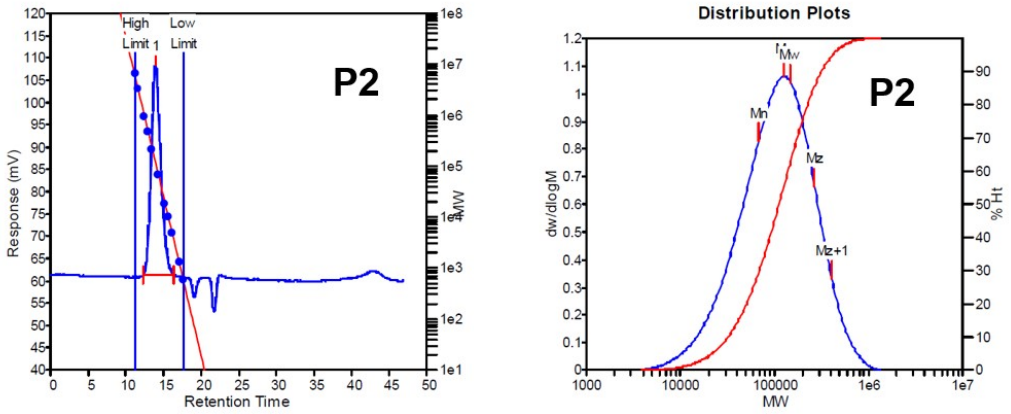

MW Averages

Peak No	Mp	Mn	Mw	Mz	Mz+1	Mv	PD
1	126263	67917	149191	267095	408019	133694	2.19667

Figure S2. GPC curve and molecular weight of **P2**.

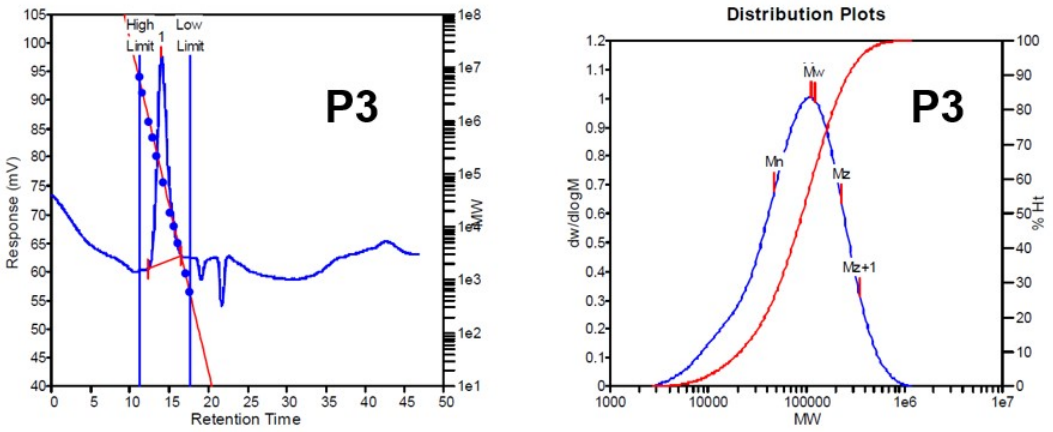

MW Averages

Peak No	Mp	Mn	Mw	Mz	Mz+1	Mv	PD
1	112001	47362	123102	229448	353140	108956	2.59917

Figure S3. GPC curve and molecular weight of **P3**.

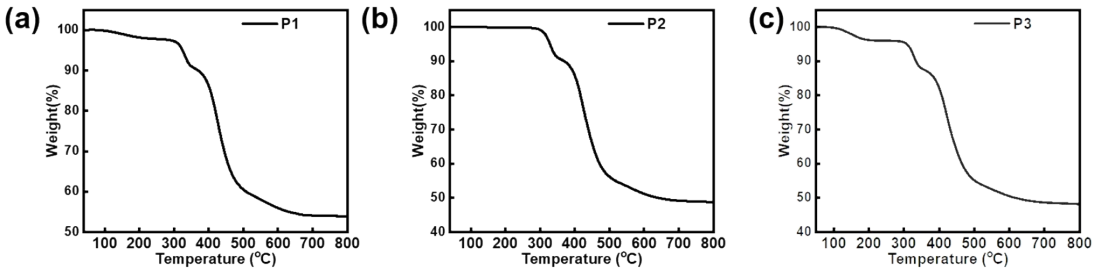

Figure S4. TGA plots of (a) **P1**, (b) **P2**, and (c) **P3** with a heating rate of 10 °C / min under an N_2 atmosphere. Temperatures with 5% weight loss for **P1**, **P2**, and **P3** are 324 °C, 328 °C, and 308 °C.

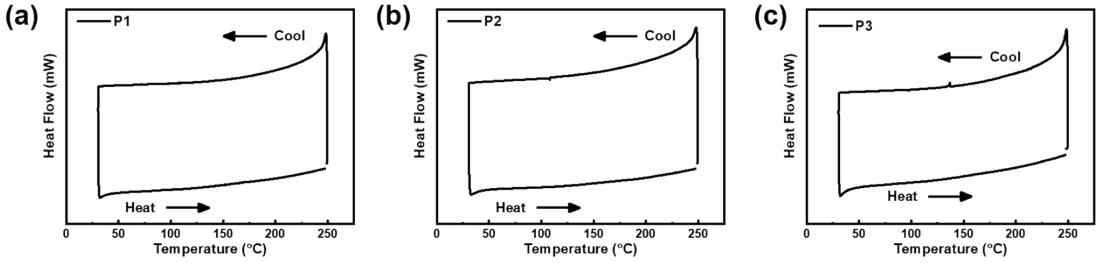

Figure S5. DSC plots of (a) **P1**, (b) **P2**, and (c) **P3**.

Table S1. The comparison of *0-0* and *0-1* transition peak intensities for donor and acceptor parts extracted from the film absorptions.

Polymers	D*0-1*	D*0-0*	D*0-0*/*0-1*	*A0-1*	A*0-0*	A*0-0*/*0-1*
P1	0.809	1	1.23	0.677	0.614	0.907
P2	0.768	1	1.30	0.754	0.709	0.940
P3	0.802	1	1.25	0.801	0.731	0.912

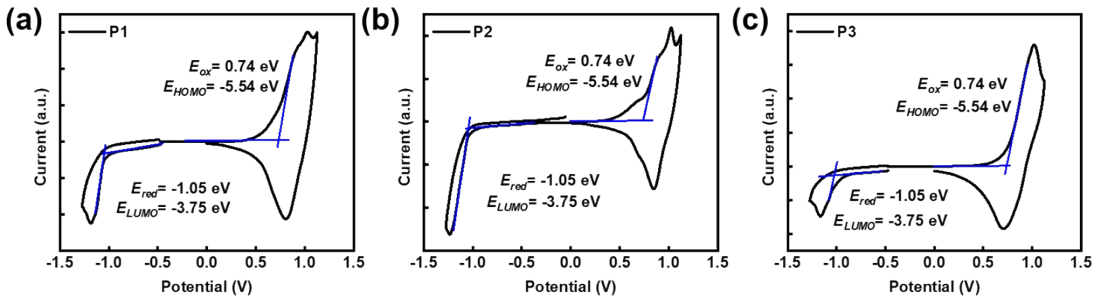

Figure S6. Cyclic voltammograms of (a) **P1**, (b) **P2**, and (c) **P3**. Potential vs. Fc/Fc^{+}.

4. Solar cells performance

Table S2. Photovoltaic performances of 6 devices based on P1 fabricated from *o*-DCB:3%DIO annealed at 150 ºC for 10 min.

No.	J_{SC} (mA/cm^2)	V_{OC} (V)	*FF*	PCE (%)
1	15.82	0.742	0.51	5.99
2	15.55	0.737	0.52	6.00
3	15.60	0.737	0.50	5.79
4	15.62	0.726	0.50	5.69
5	16.31	0.723	0.48	5.62
6	16.80	0.731	0.46	5.67
average	15.95±0.45	0.732±0.007	0.50±0.02	5.79±0.15

Table S3. Photovoltaic performances of 6 devices based on P2 fabricated from *o*-DCB:3%DIO annealed at 150 ºC for 10 min.

No.	J_{SC} (mA/cm^2)	V_{OC} (V)	*FF*	PCE (%)
1	20.17	0.738	0.63	9.45
2	20.49	0.733	0.62	9.37
3	21.05	0.732	0.61	9.42
4	19.32	0.741	0.64	9.20
5	20.61	0.734	0.61	9.27
6	21.03	0.731	0.60	9.26
average	20.44±0.59	0.734±0.003	0.62±0.01	9.32±0.09

Table S4. Photovoltaic performances of 6 devices based on P3 fabricated from *o*-DCB:3%DIO annealed at 150 ºC for 10 min.

No.	J_{SC} (mA/cm^2)	V_{OC} (V)	*FF*	PCE (%)
1	17.18	0.717	0.51	6.26
2	17.47	0.714	0.49	6.20
3	16.58	0.713	0.50	5.94
4	17.12	0.715	0.50	6.14
5	17.08	0.713	0.50	6.08
6	17.03	0.713	0.49	6.01
average	17.07±0.26	0.714±0.001	0.50±0.01	6.10±0.11

Table S5. Photovoltaic performances of 6 devices based on PBDB-T:*s*-DCPIC fabricated from *o*-DCB:3%DIO annealed at 150 ºC for 10 min.

No.	J_{SC} (mA/cm^2)	V_{OC} (V)	*FF*	PCE (%)
1	15.08	0.796	0.53	6.40
2	16.54	0.792	0.53	6.92
3	16.71	0.792	0.51	6.70
4	17.31	0.795	0.48	6.56
5	16.82	0.799	0.47	6.36
6	17.05	0.797	0.48	6.50
average	16.58±0.72	0.795±0.002	0.50±0.02	6.57±0.19

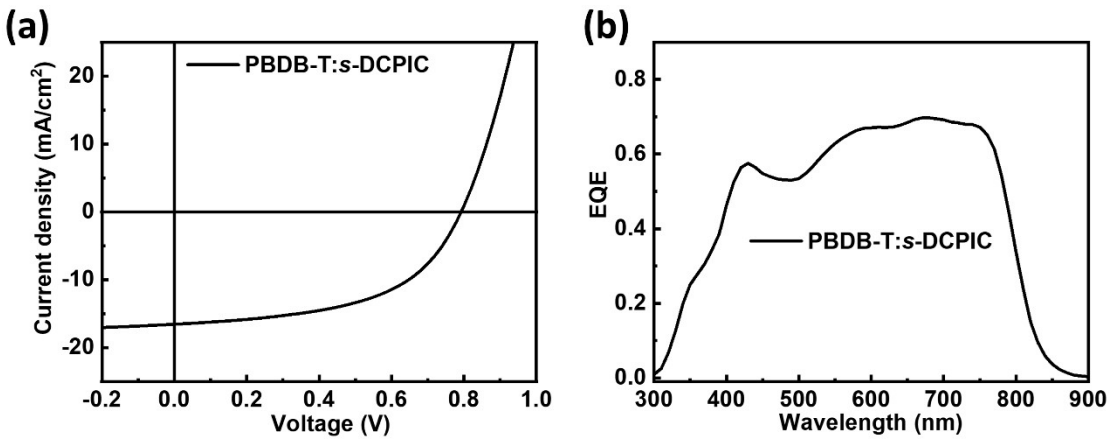

Figure S7. (a) *J*-*V* characteristics of OSCs based on PBDB-T:*s*-DCPIC. (b) The corresponding EQE spectra.

5. Thermal stability test

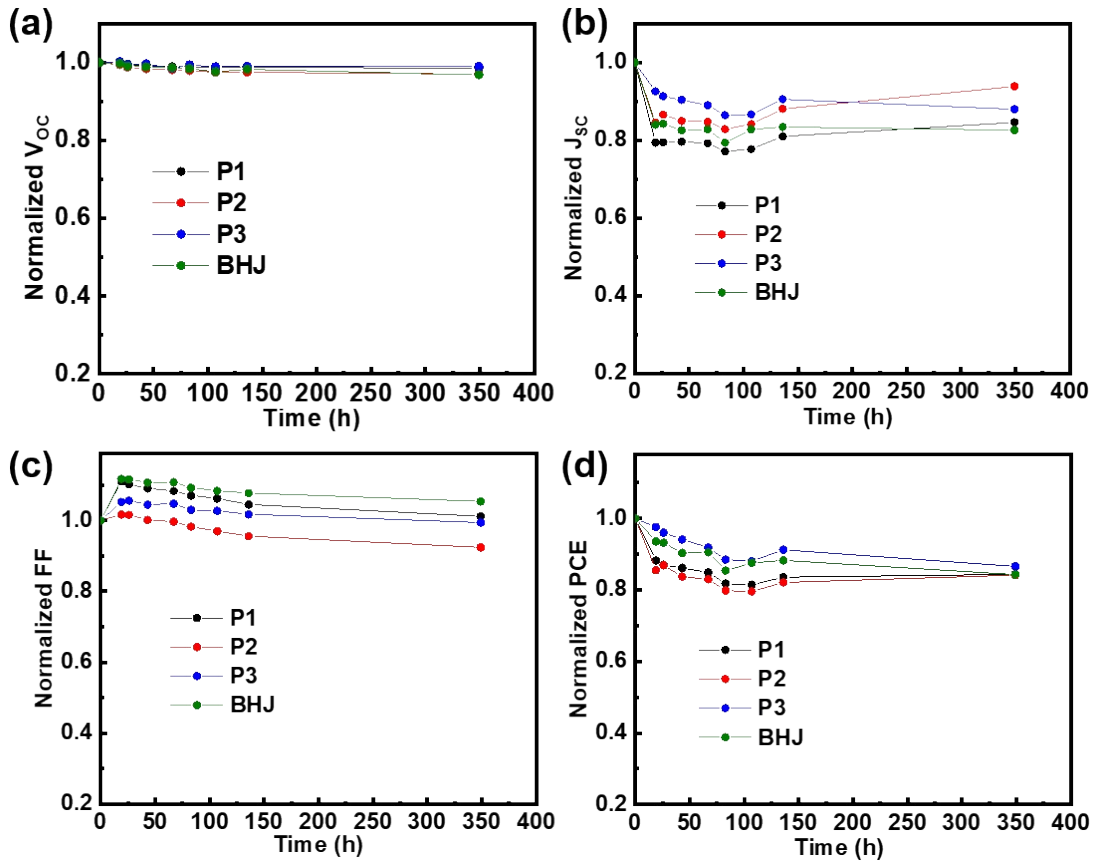

Figure S8. Thermal stability test of cells under thermal treatment at 80 ºC (dark). (a) V_{OC}, (b) J_{SC}, (c) *FF*, (d) PCE.

6. SCLC

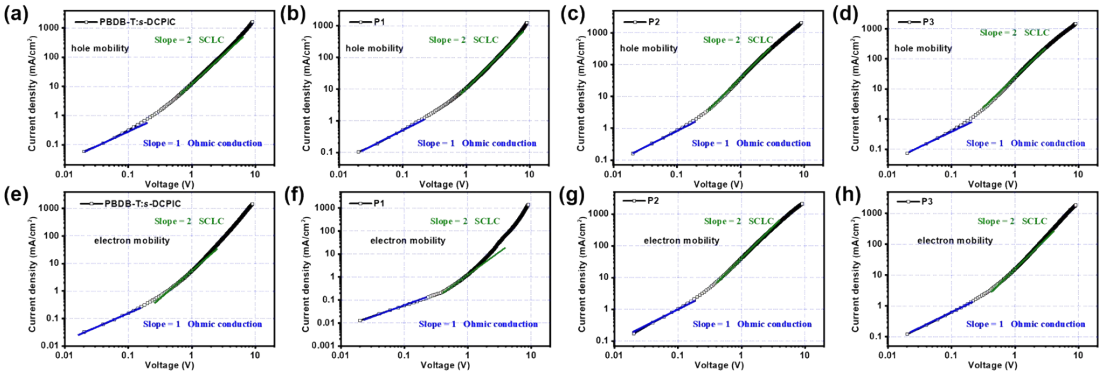

Figure S9. Hole and electron mobilities based on PBDB-T:*s*-DCPIC, **P1**, **P2,** and **P3** from SCLC measurement.

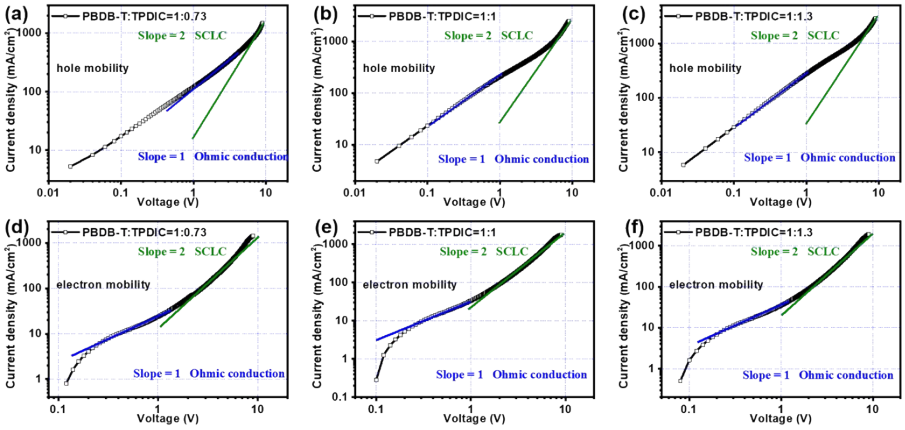

Figure S10. Hole and electron mobilities based on PBDB-T:TPDIC with different ratio from SCLC measurement.

Table S6. Charge carrier mobilities determined by SCLC measurement.

Active layers	Donor:acceptor	μ_h (cm²/V•s)	μ_e (cm²/V•s)
BHJ-1	**PBDB-T:TPDIC=1:0.73**	3.5×10^{-4}	2.6×10^{-4}
BHJ-2	**PBDB-T:TPDIC=1:1**	1.3×10^{-3}	3.9×10^{-4}
BHJ-3	**PBDB-T:TPDIC=1:1.3**	7.2×10^{-4}	4.7×10^{-4}

7. PL

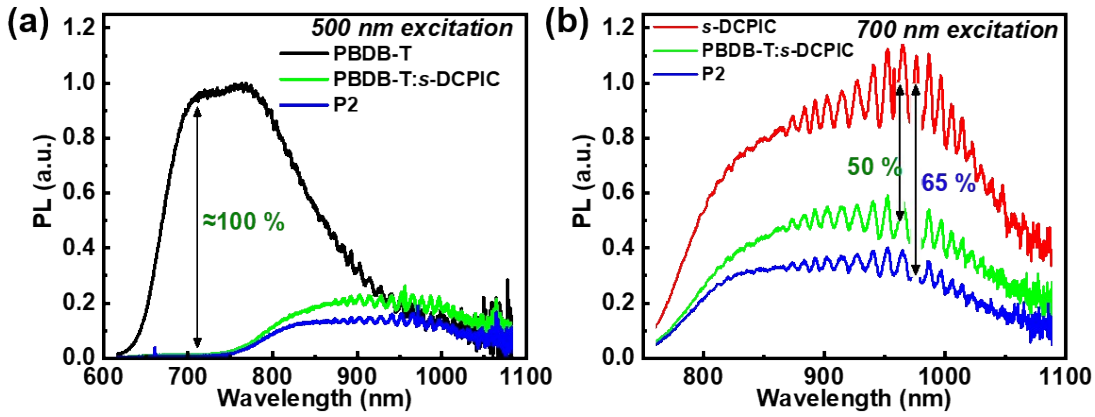

Figure S11. (a) PL spectra of PBDB-T, PBDB-T:*s*-DCPIC and P2 excited at 500 nm. (b) PL spectra of *s*-DCPIC, PBDB-T:*s*-DCPIC and P2 excited at 700 nm.

8. EQE_{EL}

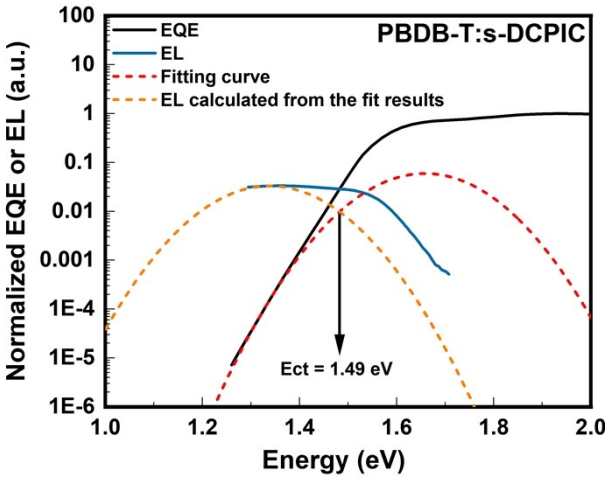

Figure S12. Normalized EQE and EL spectra of the OSCs based on PBDB-T:*s*-DCPIC.

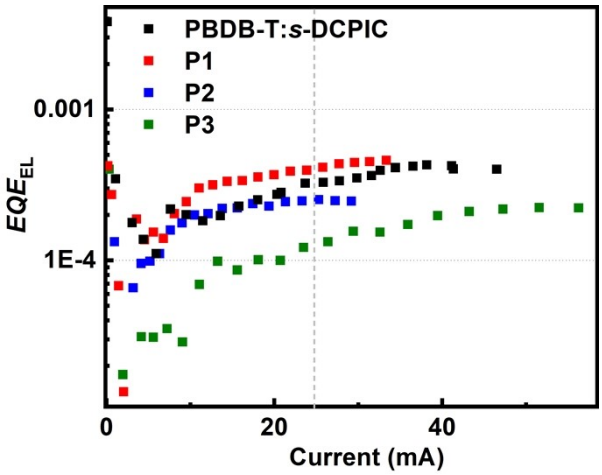

Figure S13. EQE_{EL} of OSCs based on PBDB-T:*s*-DCPIC, **P1**, **P2**, and **P3**

9. AFM and GIWAXS

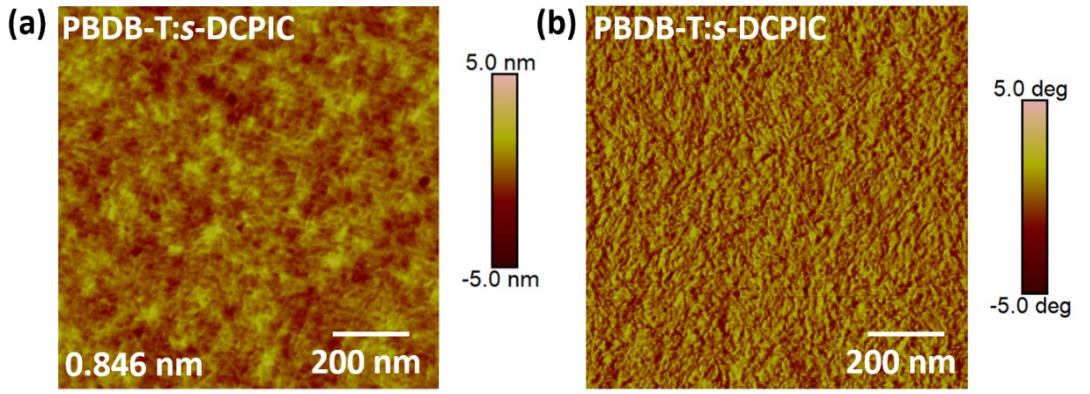

Figure S14. AFM (a) height images and (b) phase images of PBDB-T:*s*-DCPIC thin film. The number at the bottom left corner is the RMS value.

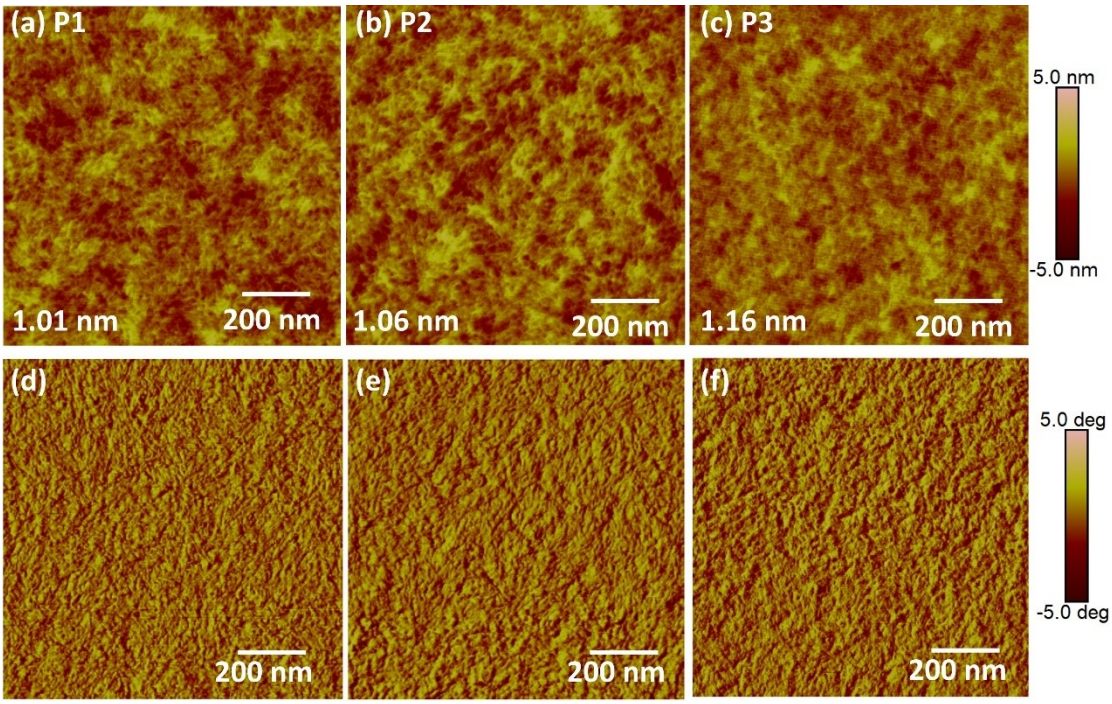

Figure S15. AFM (a-c) height images and (d-f) phase images of P1-P3 thin film. The number at the bottom left corner is the RMS values.

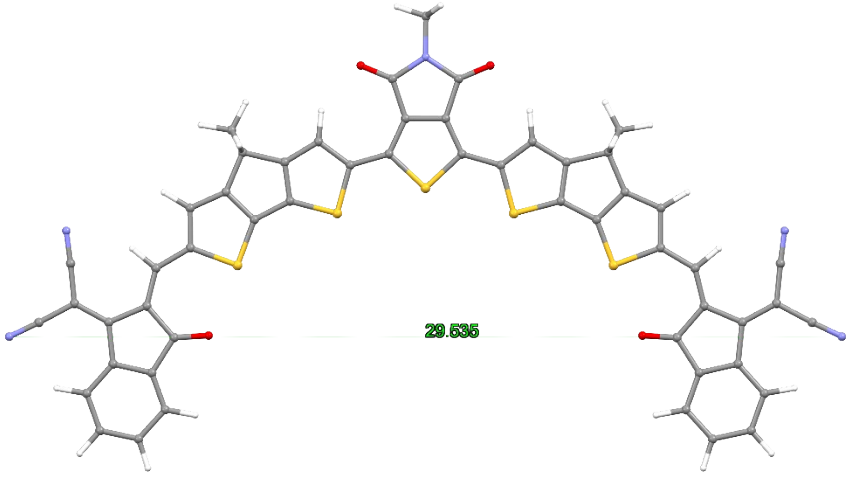

Figure S16. Optimized molecular configuration of TPDIC.

Table S7. Crystallographic parameters of the double-cable conjugated polymer thin films

Polymers	Q_4			Q_2		
	q (Å^{-1})	d (Å)	CL^a (nm)	q (Å^{-1})	d (Å)	CL^a (nm)
P1	0.650	19.33	10.8	-	-	-
P2	0.650	19.33	10.8	0.250	25.13	8.07
P3	0.650	19.33	9.5	0.244	25.75	7.78

[a]*CL* (coherence length) = $2\pi k/fwhm$, where k is a shape factor (here is 0.9).

10. Transient Absorption Spectroscopy

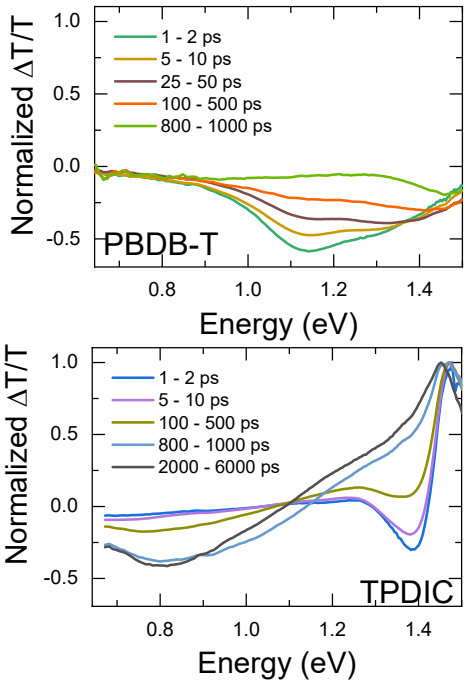

Figure S17. Normalized ps-ns TA spectra of neat PBDB-T (upper panel) TPDIC (lower panel) thin films after exciting at 650 nm.

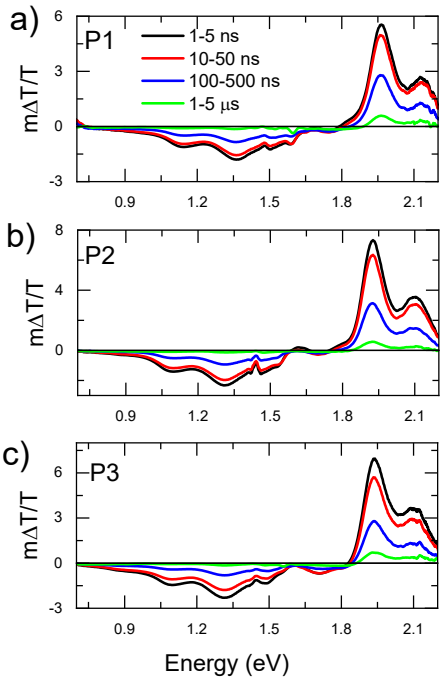

Figure S18. Nanosecond-microsecond TA spectra of (a) **P1**, (b) **P2**, and (c) **P3** after exciting at 532 nm with a fluence 4.5 μJ/cm^2.

11. NMR

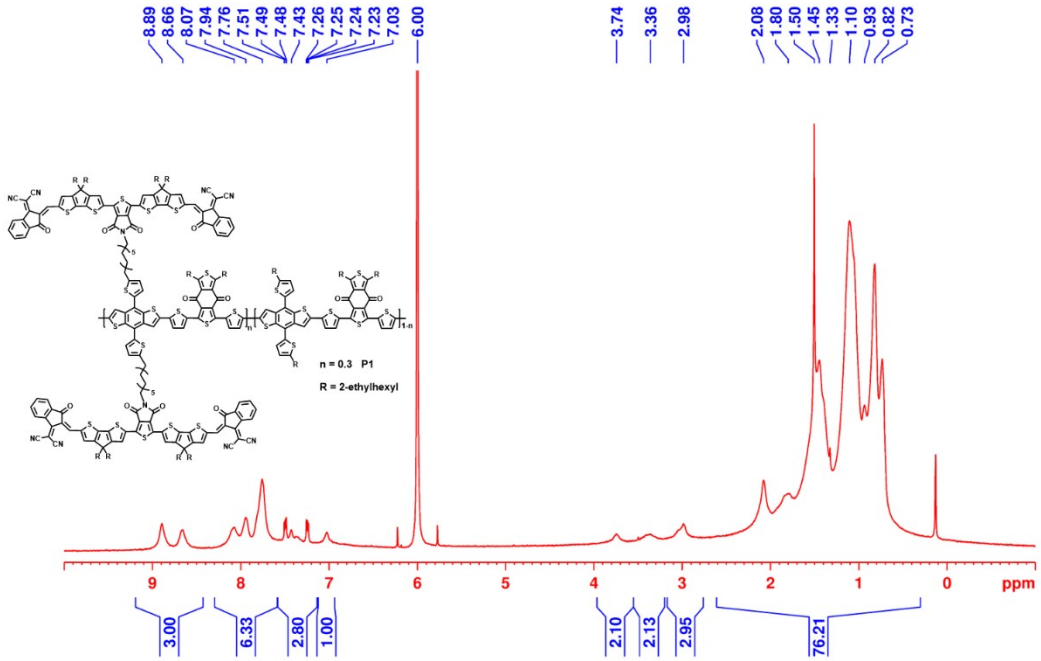

Figure S19. ^{1}H-NMR of the **P1** in 1,1,2,2-tetrachloroethane-D_2 record at 80 ºC.

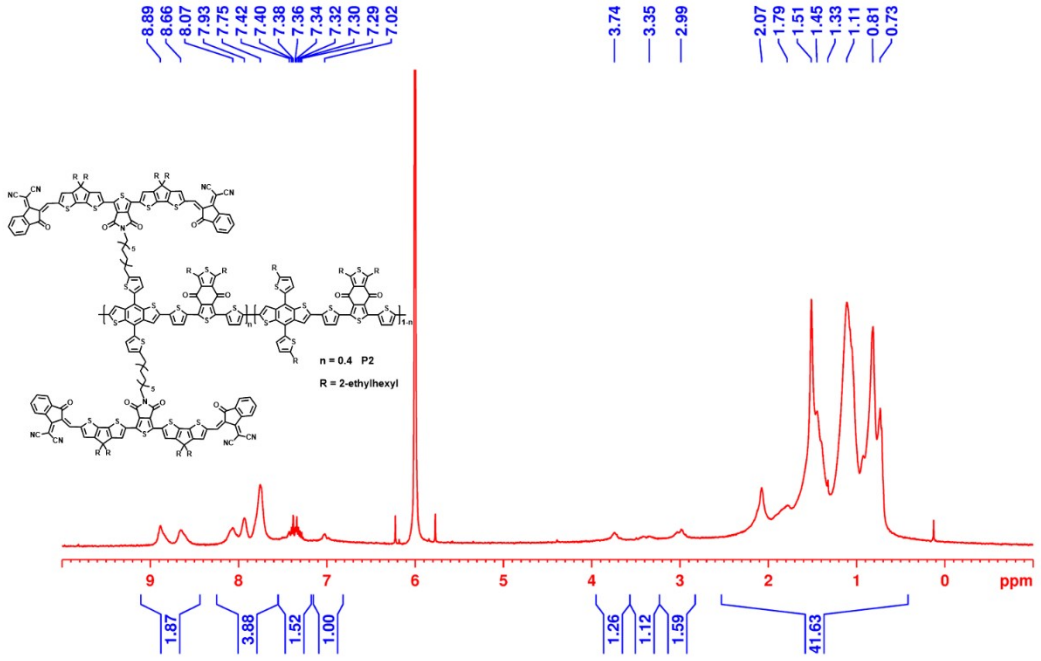

Figure S20. ^{1}H-NMR of the **P2** in 1,1,2,2-tetrachloroethane-D_2 record at 80 ºC.

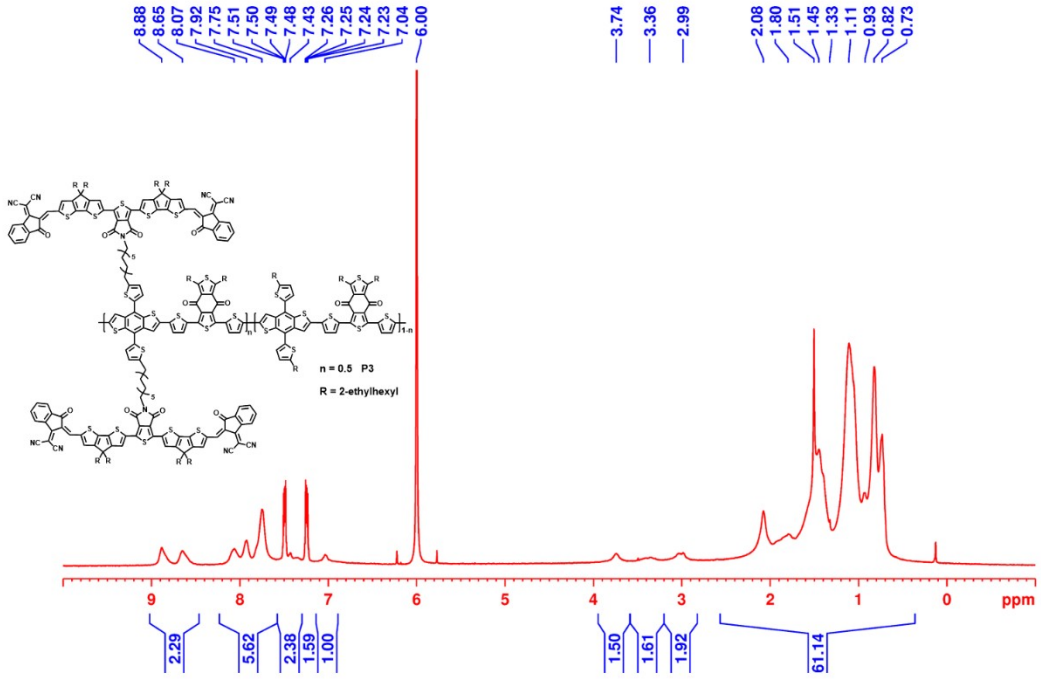

Figure S21. ^{1}H-NMR of the **P3** in 1,1,2,2-tetrachloroethane-D_2 record at 80 ºC.

12. Reference

1. S. Liang, B. Liu, S. Karuthedath, J. Wang, Y. He, W. L. Tan, H. Li, Y. Xu, N. Li, J. Hou, Z. Tang, F. Laquai, C. R. McNeill, C. J. Brabec and W. Li, *Angew. Chem. Int. Ed.*, 2022, **61**, e202209316.
2. J. Yao, B. Qiu, Z. G. Zhang, L. Xue, R. Wang, C. Zhang, S. Chen, Q. Zhou, C. Sun, C. Yang, M. Xiao, L. Meng and Y. Li, *Nat. Commun.*, 2020, **11**, 2726.
3. N. F. Mott and R. W. Gurney, *Electronic processes in ionic crystals*, Clarendon Press, 1948.
4. P. Murgatroyd, *J. Phys. D: Appl. Phys.*, 1970, **3**, 151.
5. K. Vandewal, A. Gadisa, W. D. Oosterbaan, S. Bertho, F. Banishoeib, I. Van Severen, L. Lutsen, T. J. Cleij, D. Vanderzande and J. V. Manca, *Adv. Funct. Mater.*, 2008, **18**, 2064-2070.
6. K. Vandewal, J. Widmer, T. Heumueller, C. J. Brabec, M. D. McGehee, K. Leo, M. Riede and A. Salleo, *Adv. Mater.*, 2014, **26**, 3839-3843.
7. S. Karuthedath, A. Melianas, Z. Kan, V. Pranculis, M. Wohlfahrt, J. I. Khan, J. Gorenflot, Y. Xia, O. Inganäs, V. Gulbinas, M. Kemerink and F. Laquai, *J. Mater. Chem. A*, 2018, **6**, 7428-7438.
8. A. Isakova, S. Karuthedath, T. Arnold, J. R. Howse, P. D. Topham, D. T. W. Toolan, F. Laquai and L. Luer, *Nanoscale*, 2018, **10**, 10934-10944.